

Slow waves on magnetic metamaterials and on chains of plasmonic nanoparticles: Driven solutions in the presence of retardation

O. Zhuromskyy,¹ O. Sydoruk,² E. Shamonina,^{2,a)} and L. Solymar³

¹*Institute of Optics, Information and Photonics, University of Erlangen-Nuremberg, Günther-Scharowsky-Str. 1, Bau 24, D-91058 Erlangen, Germany*

²*Erlangen Graduate School in Advanced Optical Technologies, University of Erlangen-Nuremberg, Paul-Gordan Str. 6, D-91052 Erlangen, Germany*

³*Department of Electrical and Electronic Engineering (EEE), Optical and Semiconductor Devices Group, Imperial College, Exhibition Road, London SW7 2BT, United Kingdom*

(Received 24 June 2009; accepted 14 October 2009; published online 23 November 2009)

Slow waves on chains or lattices of resonant elements offer a unique tool for guiding and manipulating the electromagnetic radiation on a subwavelength scale. Applications range from radio waves to optics with two major classes of structures being used: (i) metamaterials made of coupled ring resonators supporting magnetoinductive waves and (ii) plasmonic crystals made of nanoparticles supporting waves of near-field coupling. We derive dispersion equations of both types of slow waves for the case when the interelement coupling is governed by retardation effects, and show how closely they are related. The current distribution is found from Kirchhoff's equation by inverting the impedance matrix. In contrast to previous treatments power conservation is demonstrated in a form relevant to a finite structure: the input power is shown to be equal to the radiated power plus the powers absorbed in the Ohmic resistance of the elements and the terminal impedance. The relations between frequency and wave number are determined for a 500-element line for two excitations using three different methods. Our approach of retrieval of the dispersion from driven solutions of finite lines is relevant for practical applications and may be used in the design of metamaterials and plasmonic crystals with desired properties. © 2009 American Institute of Physics. [doi:10.1063/1.3259397]

I. INTRODUCTION

The three most important questions to be answered for any practical guiding structure are (i) how to launch the wave, (ii) how the wave propagates (what the wavelength in the guide is), and (iii) what the attenuation is. The propagation and attenuation characteristics can be rigorously calculated at least for a class of waveguides which do not radiate. Best examples are the coaxial cable and the hollow metallic waveguide in which the fields are confined within boundaries. Rigorous solutions are still available for open waveguides of infinite length, e.g., for optical fibers. The chances of finding an exact solution quickly recede when considering open periodic waveguides. An early example is a periodic array of electric dipoles¹ which was studied experimentally. For a theoretical treatment of coupled waveguides in terms of nearest neighbor interaction, see Ref. 2. Two recent examples of propagation on an array of resonant particles (see Fig. 1) are nanoparticle (NP) and magnetoinductive (MI) waves, although the physical mechanisms of the resonance are quite different. It is an *LC* resonance for the loop and a plasma resonance for the NP. The analysis to be presented here applies to both of them although they were found experimentally in entirely different frequency regions.

Waves along a linear chain of spherical metal NPs were first investigated by Quinten *et al.*³ Their motivation was

energy transport at visible frequencies by means of particles that are much smaller than the wavelength. Subsequently other aspects of these waves such as switching,⁴ splitting between longitudinal and transverse modes,⁵ radiative properties,⁶ pulse propagation,⁷ detection of electromagnetic energy,⁸ multipoles,⁹ effect on a channel waveguide,¹⁰ and two-dimensional representations¹¹ were investigated either experimentally or theoretically.

The first paper on MI waves came about as a by-product of the research on metamaterials.¹² The elements were metallic rings made resonant by inserting lumped capacitors into the rings. The initial experiments were performed in the lower megahertz region.¹³ Further analyses and experimental proofs followed.^{14–18} The properties of biperiodic and coupled MI waves were discussed^{19–22} and higher order interactions²³ were considered. Applications as waveguide components,^{24–26} transducers,²⁷ imagers,^{28–31} and nonlinear elements^{32–35} were similarly treated. For review papers, see Refs. 36 and 37.

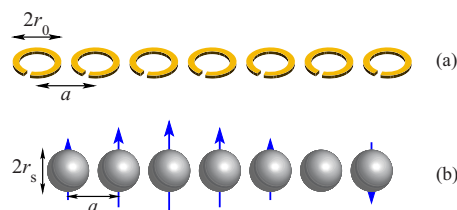


FIG. 1. (Color online) Array of coupled (a) metamaterial elements and (b) NPs both supporting slow waves.

^{a)}Author to whom correspondence should be addressed. Electronic mail: ekaterina.shamonina@aot.uni-erlangen.de.

There are a number of similarities between MI waves and NP waves. (i) Both of them have resonant elements possessing axial symmetries (loops combined with capacitances for the former, metallic nanospheres for the latter). (ii) Losses may be simply included for both of them by assuming that the metal has finite conductivity for the MI wave and an imaginary dielectric constant for the NP wave. (iii) Both of them have near-field coupling between the elements as manifested by the mutual inductance between loops for the former and the near field of an electric dipole for the latter. (iv) Both of them have two different kinds of coupling occurring when the (magnetic/electric) field is perpendicular to or parallel with the direction of propagation (these are called planar and axial configurations for MI waves and transverse and longitudinal waves for NP waves). (v) Both of them have far-field coupling as manifested by the radiation field of loops for MI waves, and the far field of electric dipoles in the transverse configuration for NP waves. (vi) Dispersion characteristics have been derived in both cases by considering coupling between (a) all the elements and (b) nearest neighbors only.

Our interest in the present paper is in the dispersion characteristics of a linear array in the presence of retardation, i.e., when all the elements are coupled to each other due to the radiation fields. The dispersion equation is supposed to tell us how the waves propagate, i.e., what the wave number q is for a given frequency ω . To find this relationship the guiding structure needs to be homogeneous, lossless and should have neither a beginning nor an end, it must be infinitely long. The derivation of the dispersion equation is fairly straightforward in principle. One needs to find the polarizability of an individual element which must include radiation damping as well. Then, conversely, the effect of all the elements upon a given element, represented by the interaction function, needs to be determined. The dispersion equation may be derived by combining these two effects (see, e.g., Refs. 38 and 39). Since the number of elements is infinite the dispersion equation appears in the form of an infinite series, each term having both real and imaginary parts. One should then specify a value for the frequency ω and find the corresponding values of the wave number q . An alternative approach is by Alu and Engheta⁴⁰ who found the dispersion equation (still for an infinite line but valid for small losses as well) in closed form in terms of polylogarithms.

Weber and Ford³⁹ had the solution for NP waves as an infinite series (both for the transverse and for the longitudinal variety) but made no attempt to solve it. Instead they chose a finite array of 20 elements. Since the coupling between the elements is known, they could determine the matrix connecting the dipole moment at element m to the excitation in element n . They found the normal modes from the condition that the matrix is singular. The method works both for the lossless and for the lossy case yielding complex values of the frequency. The disadvantage of the method of taking a finite number of elements is that only a discrete set of points can be obtained on the dispersion curve. Their most notable result is that for the transverse case the quasistatic dispersion characteristics are strongly perturbed when retardation is taken into account. They have shown that the dispersion

curves tend to the light line from both directions. In the case when retardation effects can be disregarded, as for example in a chain with strong lateral localization,⁴¹ such perturbation does not occur.

Another solution of the dispersion curve is due to Koenderink and Polman.⁴² They assumed the dipole moment in the wave form $\exp(jmqa)$, where m is an integer and a is the separation of the elements, and calculated the corresponding complex values of the frequency from the dispersion equation. They found the interesting result that the two branches, to the left and to the right of the light line, do not cross.

The lossless dispersion equation was examined by Belov and Simovski⁴³ and Simovski *et al.*⁴⁴ In the case of NP chains, the imaginary part of the interaction function exactly cancels the imaginary part (due to radiation damping) of the inverse polarizability. Thus all terms in the dispersion equation are real provided the value of q is to the right of the light line. In physical terms Belov and Simovski⁴³ argue that “the far field radiation of a single scatterer is compensated by the electromagnetic interaction in a regular three-dimensional (3D) array, so that there is no radiation loss for the wave propagating in the lattice.” This explanation, however, does not hold to the left of the light line where there are strong radiation effects.

It is generally agreed that the dispersion equation has meaning only for an infinitely long array. The arguments of Belov and Simovski⁴³ and Simovski *et al.*⁴⁴ concerning the cancellation of radiation damping are no longer valid for a finite line. Open finite structures are bound to radiate and of course all practical structures are finite. If we want to know what happens under practical conditions we must look at the way the array is excited, and find the current distribution and the corresponding radiation. The aim of this paper is, taking excitation into account, to find how the wave number varies with frequency in the presence of radiation.

We have argued in this section that MI waves and NP waves are analogous. We shall derive the dispersion characteristics for both waves in Sec. II and explore the extent of the analogy. In Sec. III we shall find the current distribution of MI waves in a 500-element array for a given value of frequency by applying the generalized Kirchhoff's equation. The relationship between frequency and wave number is then derived for two types of excitation by three different methods: Fourier analysis, input power maximization, and deduction from currents in consecutive elements. In Sec. IV we point out the difference between power conservation for an infinite line and for a finite line. Conclusions are drawn in Sec. V.

II. ANALOGY BETWEEN NP AND MI WAVES

Currents in a linear array of magnetic resonant circuits can be excited by external magnetic fields or by applying voltages to selected elements. For a 3D array it is also possible to excite the waves in the medium by an incident plane wave.⁴⁵ The voltage in element m is determined by the current in the same element and by the voltage induced by the currents flowing in all the other elements. Formally, the relationship is given by Kirchhoff's equation as follows:

$$Z_0 I_m + j\omega \sum_{l=-\infty}^{\infty} M_{ml} I_l = V_m, \quad (1)$$

where an $\exp(j\omega t)$ temporal variation is assumed, $Z_0 = j\omega L + 1/(j\omega C) + R$, L is the inductance, C is the capacitance, R is the resistance that includes both the Ohmic and the radiation parts, I_m is the current in the m th element, V_m is the voltage applied to the m th element, and M_{ml} is the mutual inductance between elements m and l . The summation is infinite for the moment although later we shall make it finite. Assuming a wave solution

$$I_m = I_0 \exp(-jqma), \quad (2)$$

substituting Eq. (2) into Eq. (1), disregarding the excitation, and using the symmetry of the situation, we find the dispersion equation after a moderate amount of algebra in the form

$$\frac{\omega_0^2}{\omega^2} = 1 - \frac{j}{Q} - 2 \sum_{n=1}^{\infty} \frac{M_n}{L} \cos(qna), \quad (3)$$

where $\omega_0 = 1/\sqrt{LC}$ is the resonant frequency and $Q = \omega L/R$ is the quality factor. For NP waves the dispersion equation can be written in the form³⁹

$$\frac{\omega^2}{\omega_0^2} = 1 + j \left(\frac{\omega\nu}{\omega_0^2} + \frac{2k^3 r_s^3}{3} \right) + 2 \frac{r_s^3}{a^3} D, \quad (4)$$

where

$$D = \sum_{n=1}^{\infty} \frac{1 + jkan - (kan)^2}{n^3} \cos(qan) \exp(-jkan), \quad (5)$$

r_s is the radius of the sphere, ω_0 is its resonant frequency, $k = \omega/c$, and c is the velocity of light.

Some simple relationships can already be seen. For the usual case of a narrow passband the two formulations agree although the left-hand sides in Eqs. (3) and (4) are reciprocal to each other. However the analogy becomes very close if we replace our capacitively loaded loops by resonant magnetic dipoles and determine the mutual inductances accordingly. It may be shown then that the terms in the infinite series are identical and the other terms are closely related. In particular, the radiation resistance of the electric dipole is replaced by the radiation resistance of the magnetic dipole.

This analogy is of practical importance. NP arrays have potential applications as subwavelength waveguides in the infrared and visible regions but they do not easily lend themselves to experimental investigations, e.g., it would be quite difficult to measure the phase and amplitude of the dipole moment on each element. Considering that experiments on MI waves could be performed with ease in the megahertz and gigahertz regions,^{13,15,18,20–23,25–31,35} it makes good sense to use MI waves as a testing ground for NP waveguide designs.

III. DRIVEN SOLUTIONS FOR MI WAVES

We shall start with a one-dimensional array of N identical resonant elements, as shown in Fig. 1(a), capable of sup-

porting MI waves. The resonant elements are capacitively loaded loops, investigated experimentally in Refs. 13, 20, and 21.

Our intention is to find the simplest model still suitable for the study of retardation effects. We wish to avoid the situation when the current in an element is no longer uniform. We have therefore chosen the size of the element to be much smaller than the wavelength. On the other hand, for retardation effects to be significant in exciting the various elements, the array has to be long relative to the wavelength. As in a previous attempt⁴⁶ our choice was a frequency of $f = \omega/(2\pi) = 0.96$ GHz, an element radius of $r_0 = 10$ mm, wire thickness of 1 mm, and distance between the elements $a = 22.5$ mm. Thus the size of the element is much smaller ($\lambda/16$) than the wavelength. The self-inductance in the metallic ring is $L = 33.1$ nH, which is made resonant at the design frequency by inserting a capacitor of $C = 0.83$ pF. We shall take here $N = 500$, which is now about 36 free space wavelengths making it clear that retardation effects will be important. To take a large number of elements is also an advantage in giving more discrete points on the dispersion characteristics.

The difficulties with the dispersion equation of the infinite line have already been pointed out in Sec. I. When a solution is found, whether in the form of an infinite series or special functions, it is still difficult to relate it to a practical problem. All practical arrays are finite and must be excited. All finite arrays radiate. We shall start with finding the current distribution first and then the relation between frequency and wave number. This relationship might differ a little from that obtained equation (3), but it is more relevant to practical cases.

Once we have a finite number of N elements it is more convenient to have a somewhat different mathematical formulation, namely, that of Eq. (1) which can be written in matrix form as

$$\mathbf{Z}\mathbf{I} = \mathbf{V}, \quad (6)$$

where \mathbf{Z} is an $N \times N$ impedance matrix. The diagonal elements correspond to the self-impedances (including the radiation resistance) and the off-diagonal elements to the real and imaginary parts of the mutual inductances.

We shall have two different kinds of excitations: (i) the first element is excited and (ii) all elements are excited by a standing wave. The two cases differ from each other only in the form of the applied voltage vector. The current distribution in both cases can be obtained by inverting the impedance matrix, yielding

$$\mathbf{I} = \mathbf{Z}^{-1}\mathbf{V}. \quad (7)$$

The inversion of a 500×500 matrix can be easily performed numerically using MATLAB.

We wish to reiterate here that the method described in this section is applicable also when all the elements are different. This includes the freedom of taking the last element different by inserting a matching impedance.

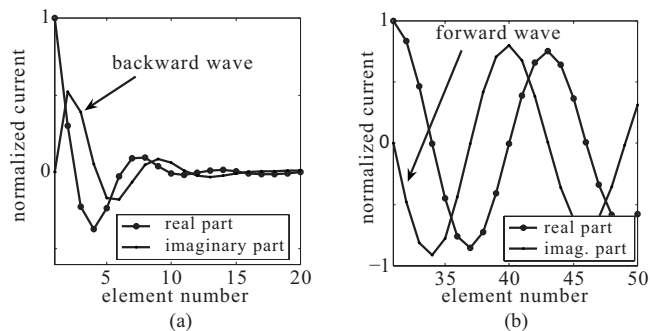


FIG. 2. (a) Real and (b) imaginary parts of the current as a function of the number of elements showing whether a wave is forward or backward.

A. Excitation by the first element

We shall now assume that only the first element of the voltage vector is different from zero and find the current distribution from Eq. (7). The current should be a declining periodic function. And this is indeed what we find in Figs. 2(a) and 2(b) where the real and imaginary parts are plotted for elements 1–20 and 30–50, respectively. We may conclude that the wave is a backward wave at the beginning of the line and turns into a forward wave as it propagates down the line. The explanation is that two waves are simultaneously excited: a large-amplitude, high-attenuation backward wave and a low-amplitude, low-attenuation forward wave, similar to that found in Ref. 46. The backward wave vanishes by the 20th element and only the forward wave propagating close to the velocity of light survives.

We can repeat the exercise for a number of Q values. As Q increases losses decrease and the amplitude decline is more gradual. This is shown in Fig. 3 for $Q=100, 1000, 2500,$ and 5000 . The phase against element number also depends strongly on the value of Q , as shown in Fig. 4, for $Q=100, 1000, 2000, 3000, 4000,$ and 5000 . We can see again that as losses are lower the backward wave dominates further away in the line. An alternative way of extracting the information is to find the Fourier components of the current distribution which for small losses is a good approximation. We have done it by using the FFT MATLAB program. Thus we may find the real part of the wave number q' (or wave numbers if there are more than one) for any value of frequency. Repeating the exercise for 220 values of the frequency and four values of the quality factor, $Q=100, 1000, 10\,000,$ and

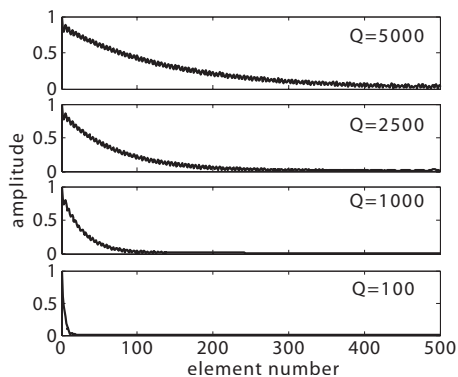


FIG. 3. Decay of current amplitude as a function of element number.

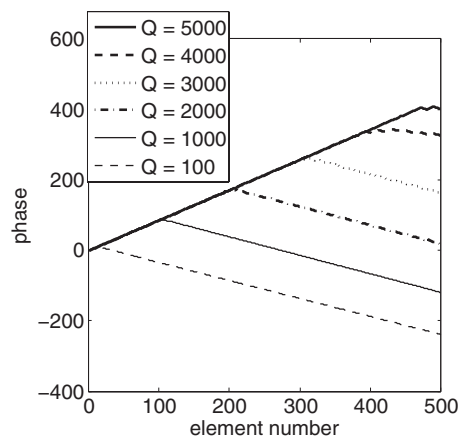


FIG. 4. Variation in the phase of the current as a function of element number.

∞ , we have four curves, as shown in Figs. 5(a)–5(d), as contour plots. For a given value of ω we find a spread in the corresponding q' values. The amount of the spread depends, as may be expected, on the value of Q . For $Q=10\,000$ and infinity the lines are quite narrow so they should be close to the “true” dispersion curve. For $Q=10\,000$ there is a just discernible curve in the range $1 < q'a/\pi < 2$. For $Q=\infty$ the curve is clearly visible. The reason is that without a matched load there is a nearly perfect reflection from the end of the array; hence, in the presence of low Ohmic losses, the q' values are about the same in both directions.

The spread in the wave vector was shown in order to appreciate how narrow (or wide) the Fourier spectrum is. Taking the maxima of the spectrum, an unambiguous dispersion curve is obtained for each value of Q , as shown in Figs. 6(a)–6(d). The new feature shown is the convergence of the curve to the light line for $Q=10\,000$ and ∞ , which means that another solution exists (represented by a local maximum) as well. It could not be seen in Figs. 6(a) and 6(b) because their values were too small. This is in line with the conclusions arrived at earlier in this section. There are two waves excited, a backward wave and a forward wave, the latter one propagating close to the velocity of light.

The relation between the wave number q and the frequency ω can be found by yet another method. Assuming that the line is able to propagate L waves with the wave numbers q_l , we can write the current in the m th element of the line in the general form,²⁰

$$I_m = \sum_{l=1}^L [I_{0l}^{(t)} \exp(-jq_l am) + I_{0l}^{(r)} \exp(jq_l am)], \quad (8)$$

where the superscripts (t) and (r) refer to the transmitted and reflected waves. At each frequency, the values of $q_l, I_{0l}^{(t)},$ and $I_{0l}^{(r)}$ can be found from the values of currents in $3L$ consecutive elements.²⁰ Note that the wave numbers q_l are assumed to be complex, and this method allows to extract the dispersion characteristics also in the presence of loss.

As seen in Fig. 6(d), there are two propagating waves in the frequency band from $0.985\omega_0$ to $1.011\omega_0$, so it is sufficient to take $L=2$ in Eq. (8). The resulting dispersion relation is shown in Fig. 7. The dispersion was extracted from the

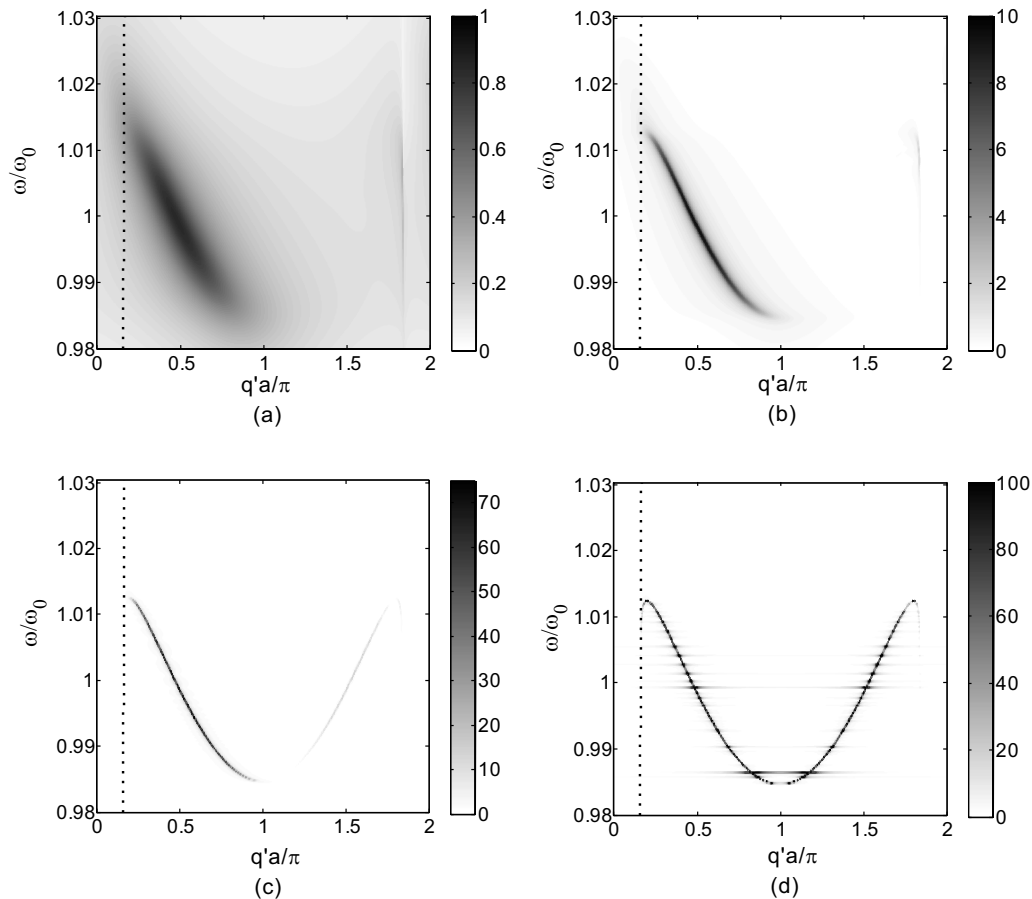


FIG. 5. Magnitude and distribution of the Fourier components plotted in the normalized ω vs $q'a/\pi$ plane for four different values of the quality factor: [(a)–(d)] $Q=100, 1000, 10\,000$, and ∞ .

currents in the 500-element line with $Q=\infty$ starting from the 250th element. Similar dispersion curves were extracted starting from different elements sufficiently far from the line ends. The dispersion curves of Fig. 7 are the same as those of Fig. 6(d) between $0.985\omega_0$ and $1.011\omega_0$. Outside this band, the dispersion curves follow the light line.

B. Excitation by standing waves

An alternative method relies on excitation of the spatial resonances. This is accomplished by applying voltages to each element of the array, such that the voltage amplitudes follow the amplitudes of the standing wave patterns. In order to excite the s -order resonance (s is the number of the half MI wavelengths in the resonator) the voltage amplitudes can take the form

$$V_m = V_0 \sin \frac{sm\pi}{N+1}, \quad (9)$$

where m is the element number, V_0 is the constant voltage, which for simplicity is chosen to be 1 V, and N is the number of resonators in the array. The number of possible spatial resonances coincides with the number of elements in the array, which is 500 in our case. For every spatial harmonics a frequency scan is performed. Excitations with the temporal and spatial frequencies close to the dispersion line will be excited most efficiently. We have chosen the input power as a measure for this efficiency,

$$P_{\text{in}} = \frac{1}{2} \sum_{m=1}^N \text{Re}(V_m I_m^*), \quad (10)$$

where the summation is over all the elements in the array. The numerical work is now much easier to perform because the impedance matrix has already been inverted when single-element excitation was considered. Taking now excitation in the form of Eq. (9) the dependence of the input power on frequency and wave number is presented in Figs. 8(a)–8(d) in the form of contour plots for $Q=100, 1000, 10\,000$, and ∞ . The spread may be seen to decline as the quality factor increases. The positions of the maxima are the same in all four cases. They are plotted in Fig. 9. The dispersion curves obtained from the propagating and standing wave excitations for the lossless elements are compared in Fig. 10. To the right of the light line the agreement is excellent. There is some discrepancy to the left of the light line presumably for the reason that the radiation patterns are quite different for the two excitations and that it has an effect upon the ω – q relationship.

The fact that the three different approaches to the dispersion equation yield practically identical results gives us confidence that each one of them is built on solid physical foundations.

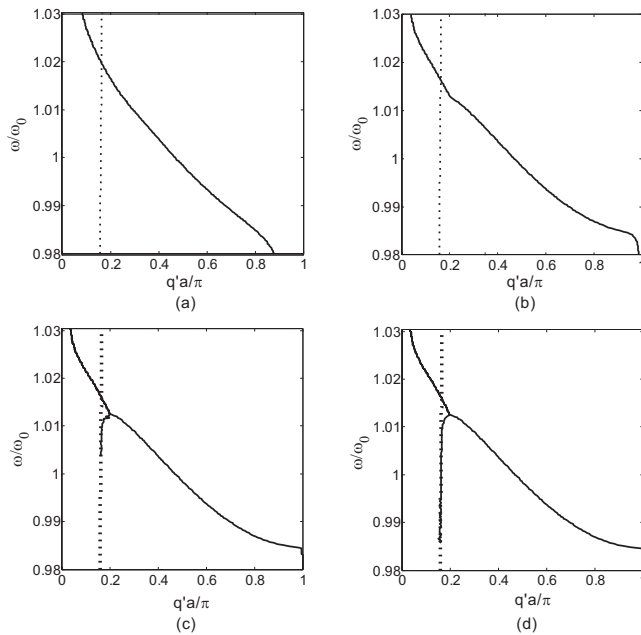


FIG. 6. Dispersion characteristics obtained from the positions of the maxima of the Fourier amplitudes. The plots (a)–(d) correspond to the four values of the quality factor: $Q=100, 1000, 10\,000,$ and ∞ .

IV. A NOTE ON POWER CONSERVATION

It is far from obvious that a model describing both guiding and radiation effects for a finite array will necessarily lead to power conservation, particularly so when there are several power absorbing mechanisms. Altogether there are four different powers to consider: (i) the input power, (ii) the power absorbed in the elements due to Ohmic losses, (iii) the power absorbed in a terminal impedance, and (iv) the radiated power. Power conservation means that the input power is equal to the sum of the other three.

There are several points to emphasize here. All the treatments of NP waves we know of have considered neither input power nor terminal impedances. First, they did not consider excitations by applied voltages, and second, they could not consider terminal impedances because it makes little sense if the array is infinitely long. Similar arguments apply to radiating power. As shown by Belov and Simovski⁴³ and

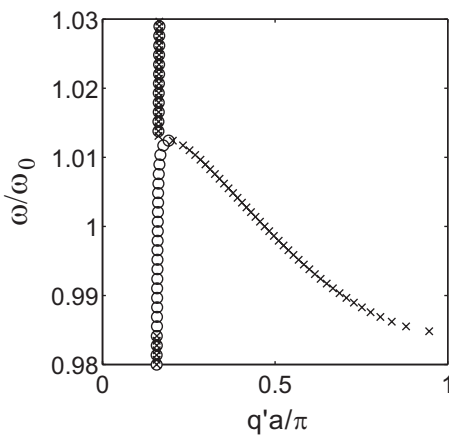


FIG. 7. Dispersion curves obtained from the values of the currents in elements 250–255 of the 500-element line assuming two propagating waves.

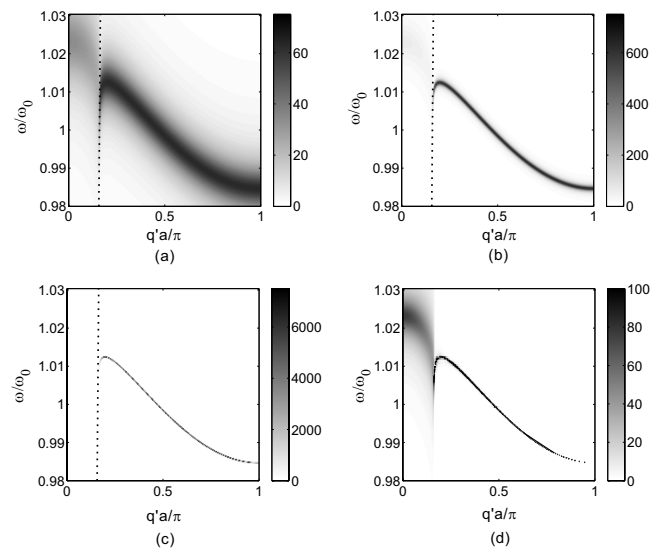


FIG. 8. Input power in a line consisting of 500 elements for quality factors (a) 100, (b) 1000, (c) 10 000, and (d) infinity. Each element of the line is excited with a voltage such that the voltages mimic one of the standing waves.

Simovski *et al.*⁴⁴ for an infinite array and mentioned in Sec. I, there is no radiation in the guided wave region due to a delicate canceling mechanism. However the situation is quite different for a finite array. Once the array is finite and open to air, and currents flow in the elements, there will be a field in any of the points of 3D space due to each element, which need to be added up in phase to obtain the far field. The radiated power may then be obtained by integrating the radiated power density over a sphere in the far field.

We have investigated numerically power conservation in the sense mentioned above for a large number of parameters and terminal impedances. Power was found to be conserved in each case to a high degree of accuracy. If we replace our capacitively loaded loops by resonant magnetic dipoles, then the power conservation can be shown analytically. However some care needs to be exercised. If in our numerical study of power conservation we take the mutual inductances as calculated for loops of finite size but take the radiation resistance as that of a magnetic dipole, then power conservation

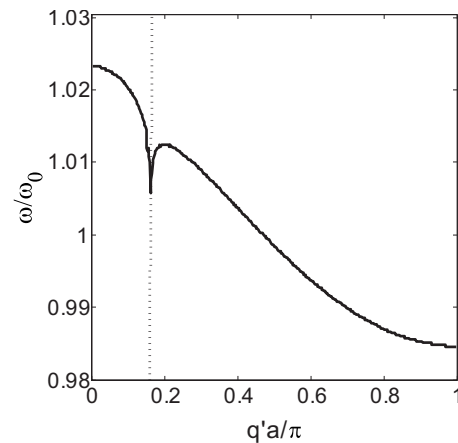


FIG. 9. Dispersion curve for $Q=1000$ derived from the criterion of maximum input power.

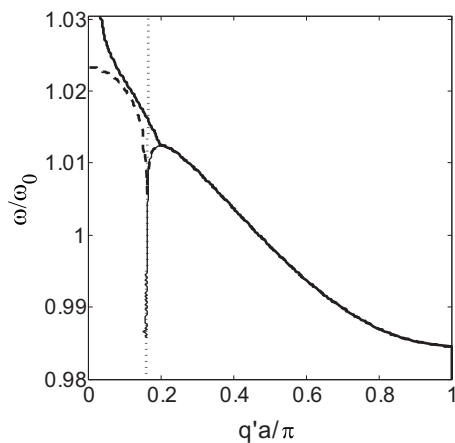


FIG. 10. Comparison of the dispersion curves obtained by single-element excitation (solid line) and standing-wave excitation (dashed line).

may be violated by as much as 20%. Proper power conservation is obtained only if the radiation resistance is recalculated by integrating the radiation field of a single loop.

V. CONCLUSIONS

The dispersion characteristics of both MI and NP waves have been derived and shown to be analogous provided the passband of the waves is narrow. It has been argued that the dispersion equations derived from driven solutions for a finite array are more relevant for practical applications than those derived from the infinite series. It is suggested that the analogy between MI and NP waves could be exploited for using MI waves as a testing ground for NP waveguide design.

Two kinds of driven solutions are considered for a MI line consisting of 500 elements: first, with the excitation of the first element, and second, with a standing wave excitation. The relation between the frequency and the wave number is obtained by three different methods: Fourier analysis, optimization of input power, and deduction from the currents in consecutive elements. All three methods have been shown to give very similar results.

Power conservation has been shown to apply. The input power is equal to the sum of powers lost by resistive and radiative effects plus the loss in a terminal impedance.

ACKNOWLEDGMENTS

O.Z., O.S., and E.S. gratefully acknowledge the funding of the German Research Foundation (Emmy Noether-Programme and SAOT).

¹J. Shefer, *IEEE Trans. Microwave Theory Tech.* **11**, 55 (1963).

²R. R. A. Syms, *IEEE J. Quantum Electron.* **23**, 525 (1987).

³M. Quinten, A. Leitner, J. R. Krenn, and F. R. Aussenegg, *Opt. Lett.* **23**, 1331 (1998).

⁴M. L. Brongersma, J. W. Hartman, and H. A. Atwater, *Phys. Rev. B* **62**, R16356 (2000).

⁵S. A. Maier, P. G. Kik, and H. A. Atwater, *Appl. Phys. Lett.* **81**, 1714 (2002).

⁶V. Yannopoulos and N. V. Vitanov, *Phys. Rev. Lett.* **99**, 053901 (2007).

⁷S. A. Maier, P. G. Kik, and H. A. Atwater, *Phys. Rev. B* **67**, 205402 (2003).

⁸S. A. Maier, P. G. Kik, H. A. Atwater, S. Meltzer, E. Hatrel, B. E. Koel, and A. G. Requicha, *Nature Mater.* **2**, 229 (2003).

⁹S. Y. Park and D. Stroud, *Phys. Rev. B* **69**, 125418 (2004).

¹⁰R. Quidant, C. Girard, J.-C. Weeber, and A. Dereux, *Phys. Rev. B* **69**, 085407 (2004).

¹¹S. A. Maier, M. D. Friedman, P. E. Barclay, and O. Painter, *Appl. Phys. Lett.* **86**, 071103 (2005).

¹²E. Shamonina, V. A. Kalinin, K. H. Ringhofer, and L. Solymar, *Electron. Lett.* **38**, 371 (2002).

¹³M. C. K. Wiltshire, E. Shamonina, I. R. Young, and L. Solymar, *Electron. Lett.* **39**, 215 (2003).

¹⁴E. Shamonina, V. A. Kalinin, K. H. Ringhofer, and L. Solymar, *J. Appl. Phys.* **92**, 6252 (2002).

¹⁵M. C. K. Wiltshire, E. Shamonina, I. R. Young, and L. Solymar, *J. Appl. Phys.* **95**, 4488 (2004).

¹⁶O. Zhuromskyy, E. Shamonina, and L. Solymar, *Opt. Express* **13**, 9299 (2005).

¹⁷R. R. A. Syms, E. Shamonina, and L. Solymar, *Eur. Phys. J. B* **46**, 301 (2005).

¹⁸R. R. A. Syms, I. R. Young, and L. Solymar, *J. Phys. D* **39**, 3945 (2006).

¹⁹O. Sydoruk, O. Zhuromskyy, E. Shamonina, and L. Solymar, *Appl. Phys. Lett.* **87**, 072501 (2005).

²⁰O. Sydoruk, A. Radkovskaya, O. Zhuromskyy, E. Shamonina, M. Shamonin, C. J. Stevens, D. J. Edwards, G. Faulkner, and L. Solymar, *Phys. Rev. B* **73**, 224406 (2006).

²¹A. Radkovskaya, O. Sydoruk, M. Shamonin, C. J. Stevens, G. Faulkner, D. J. Edwards, E. Shamonina, and L. Solymar, *IET Proc. Microwaves, Antennas Propag.* **1**, 80 (2007).

²²A. Radkovskaya, O. Sydoruk, M. Shamonin, C. J. Stevens, G. Faulkner, D. J. Edwards, E. Shamonina, and L. Solymar, *Microwave Opt. Technol. Lett.* **49**, 1054 (2007).

²³R. R. A. Syms, O. Sydoruk, E. Shamonina, and L. Solymar, *Metamaterials* **1**, 44 (2007).

²⁴E. Shamonina and L. Solymar, *J. Phys. D* **37**, 362 (2004).

²⁵R. R. A. Syms, L. Solymar, and E. Shamonina, *IEEE Proc. Microwaves, Antennas Propag.* **152**, 77 (2005).

²⁶R. R. A. Syms, E. Shamonina, and L. Solymar, *IEEE Proc. Microwaves, Antennas Propag.* **153**, 111 (2006).

²⁷M. J. Freire, R. Marques, F. Medina, M. A. G. Laso, and F. Martin, *Appl. Phys. Lett.* **85**, 4439 (2004).

²⁸M. J. Freire and R. Marques, *Appl. Phys. Lett.* **86**, 182505 (2005).

²⁹M. J. Freire and R. Marques, *J. Appl. Phys.* **100**, 063105 (2006).

³⁰O. Sydoruk, M. Shamonin, A. Radkovskaya, O. Zhuromskyy, E. Shamonina, R. Trautner, C. J. Stevens, G. Faulkner, D. J. Edwards, and L. Solymar, *J. Appl. Phys.* **101**, 073903 (2007).

³¹M. J. Freire and R. Marques, *J. Appl. Phys.* **103**, 013115 (2008).

³²I. V. Shadrivov, A. A. Zharov, and Y. S. Kivshar, *Appl. Phys. Lett.* **83**, 2713 (2003).

³³O. Sydoruk, V. A. Kalinin, and E. Shamonina, *Phys. Status Solidi B* **244**, 1176 (2007).

³⁴O. Sydoruk, E. Shamonina, and L. Solymar, *J. Phys. D* **40**, 6879 (2007).

³⁵R. R. A. Syms, *Metamaterials* **2**, 122 (2008).

³⁶E. Shamonina and L. Solymar, *J. Magn. Magn. Mater.* **300**, 38 (2006).

³⁷E. Shamonina and L. Solymar, *Metamaterials* **1**, 12 (2007).

³⁸S. A. Tretyakov, *Analytical Modeling in Applied Electromagnetics* (Artech House, Boston, 2003).

³⁹W. H. Weber and G. W. Ford, *Phys. Rev. B* **70**, 125429 (2004).

⁴⁰A. Alu and N. Engheta, *Phys. Rev. B* **74**, 205436 (2006).

⁴¹G. Gantzounis and N. Stefanou, *Phys. Rev. B* **74**, 085102 (2006).

⁴²A. F. Koenderink and A. Polman, *Phys. Rev. B* **74**, 033402 (2006).

⁴³P. A. Belov and C. R. Simovski, *Phys. Rev. E* **72**, 036618 (2005).

⁴⁴C. R. Simovski, A. J. Viitanen, and S. A. Tretyakov, *Phys. Rev. E* **72**, 066606 (2005).

⁴⁵P. A. Belov and C. R. Simovski, *Phys. Rev. B* **73**, 045102 (2006).

⁴⁶O. Zhuromskyy, E. Shamonina, and L. Solymar, *Proc. SPIE* **5955**, 595506 (2005).